



# Enhancing ceria slurry performance for shallow trench isolation chemical mechanical polishing through non-ionic surfactant addition

Lifei Zhang<sup>1</sup> · Lile Xie<sup>1</sup> · Xinchun Lu<sup>1</sup>

Received: 10 March 2023 / Accepted: 27 August 2023 / Published online: 5 September 2023  
© The Author(s), under exclusive licence to Springer-Verlag London Ltd., part of Springer Nature 2023

## Abstract

Chemical mechanical polishing (CMP) is a committed step in the manufacturing of integrated circuits, especially in the fabrication process of shallow trench isolation (STI) structures. Ceria ( $\text{CeO}_2$ ) slurry is widely used in the STI CMP process, while it is vulnerable to causing surface defects owing to particle agglomeration, such as scratches and abrasive residues. Furthermore,  $\text{CeO}_2$  slurry faces the challenge of low polishing removal selectivity between silicon dioxide ( $\text{SiO}_2$ ) and silicon nitride ( $\text{Si}_3\text{N}_4$ ) surfaces. In this study, we investigated the effects of various non-ionic surfactants and different pH levels in  $\text{CeO}_2$ -based slurries on material removal rates, removal selectivity, and surface qualities of polished wafers. Two of the studied non-ionic surfactants that make  $\text{CeO}_2$  slurries disperse better were selected through sedimentation experiments, which were polyethylpyrrolidone (PVP-K30) and polyethylene glycol, respectively. Subsequently, polishing experiments and atomic force microscopy characterization tests were conducted to illustrate the effects of the selected surfactants at different pH conditions. To further explore the underlying mechanism, the reaction of surfactants on  $\text{SiO}_2$  and  $\text{Si}_3\text{N}_4$  wafers was explained using surface adsorption tests, thermogravimetry experiments, zeta potential measurements, and chemical valence bond structure analysis. As a result, it can be concluded that the performance of ceria slurries used in STI CMP process can be improved by the addition of non-ionic surfactant PVP-K30.

**Keywords** Shallow trench isolation · Chemical mechanical polishing · Ceria slurry · Non-ionic surfactants · Polyethylpyrrolidone

## 1 Introduction

Shallow trench isolation (STI), the most frequently used device isolation technology today, is an approach to achieve isolation by etching the silicon substrate who has a topped layer of silicon nitride ( $\text{Si}_3\text{N}_4$ ), to form an isolation trench and fill it with insulating dielectric such as silicon dioxide ( $\text{SiO}_2$ ) [1]. Chemical mechanical polishing (CMP) is considered as the indispensable planarization technique in

integrated circuit manufacturing and a key step in the fabrication of STI structures [2]. In the CMP process of STI, compared with the traditional silica slurries, ceria ( $\text{CeO}_2$ ) slurries have a higher material removal rate on  $\text{SiO}_2$  and greater removal selectivity between  $\text{SiO}_2$  and  $\text{Si}_3\text{N}_4$ , while it is still insufficient to meet the strict specification that the removal selection ratio between  $\text{SiO}_2$  and  $\text{Si}_3\text{N}_4$  is supposed to be greater than 20:1 [3–5]. Therefore, the preparation and modification of ceria slurries have been becoming a popular research topic.

The material removal rate (MRR) of  $\text{Si}_3\text{N}_4$  can be controlled by introducing appropriate surfactants into  $\text{CeO}_2$ -based slurries, thus achieving high selectivity [6]. Generally, compared with ionic surfactants, non-ionic surfactants have two distinct advantages: first, non-ionic surfactants have an ability to maintain or even improve the removal selectivity between  $\text{SiO}_2$  and  $\text{Si}_3\text{N}_4$  while inhibiting the removal of  $\text{Si}_3\text{N}_4$ ; second, the use of non-ionic surfactants can enhance the stability of  $\text{CeO}_2$  slurries and thus improve the surface qualities of polished  $\text{SiO}_2$  and  $\text{Si}_3\text{N}_4$ . Cho

Lifei Zhang and Lile Xie are equal contributors.

✉ Xinchun Lu  
xclu@tsinghua.edu.cn

Lifei Zhang  
zlf16@tsinghua.org.cn

Lile Xie  
ll-xie15@tsinghua.org.cn

<sup>1</sup> State Key Laboratory of Tribology in Advanced Equipment, Tsinghua University, Beijing 100084, China

et al. [7] demonstrated that the introduction of the surfactant polyacrylic acid in  $\text{CeO}_2$ -based slurries can strongly reduce  $\text{Si}_3\text{N}_4$  MRRs, through adsorbing only on  $\text{Si}_3\text{N}_4$  surfaces and thus forming a dense passivation layer to control the removal selectivity between  $\text{SiO}_2$  and  $\text{Si}_3\text{N}_4$ . Veera et al. [8] showed that at pH values of 4 and 5, cyclic amine surfactants, namely pyridine HCl, piperazine, and imidazole, could effectively decrease  $\text{Si}_3\text{N}_4$  MRRs without affecting the removal rates of  $\text{SiO}_2$ . Praveen et al. [9] added surfactants l-glutamic acid and l-proline into a synthesized  $\text{CeO}_2$ -based slurries, both of which could achieve high selectivity between  $\text{SiO}_2$  and  $\text{Si}_3\text{N}_4$ . However, the current research on non-ionic surfactants has several deficiencies that the qualities of polished  $\text{SiO}_2$  and  $\text{Si}_3\text{N}_4$  surfaces which directly affect the following fabricating process are inadequate, including the number and depth of scratches, as well as surface roughness. Moreover, the explanation of the action mechanism mainly focuses on the adsorption of  $\text{SiO}_2$  and  $\text{Si}_3\text{N}_4$  wafer surfaces, but ignores the effect of surfactants on zeta potentials of  $\text{CeO}_2$  particles and other aspects. On the other hand, pH levels also play a crucial role in removal rates and corresponding selectivity between  $\text{SiO}_2$  and  $\text{Si}_3\text{N}_4$  surfaces [10–12]. Manivannan et al. [10] found that a  $\text{CeO}_2$  based slurry with DL-aspartic acid could present high removal selectivity between  $\text{SiO}_2$  and  $\text{Si}_3\text{N}_4$  only in the pH ranges of 4 to 5, where at low pH values, the removal rates of  $\text{SiO}_2$  and  $\text{Si}_3\text{N}_4$  were slow, whereas at high pH conditions, the removal rates of  $\text{SiO}_2$  and  $\text{Si}_3\text{N}_4$  were not significantly inhibited. Supphantharida et al. [11] found that with the increase of pH, silicate adsorption first increases and then decreases, reaching a maximum at about pH 9, and this adsorption may directly participate in the removal mechanism of  $\text{SiO}_2$  and  $\text{Si}_3\text{N}_4$  in the CMP process. Kim et al. [12] demonstrated that pH values affect the colloidal interactions between anionic polyelectrolyte additives and  $\text{SiO}_2/\text{Si}_3\text{N}_4$  surfaces, with the maximum selectivity obtained for  $\text{SiO}_2$  and  $\text{Si}_3\text{N}_4$  at pH 7.

In order to enhance the stability of  $\text{CeO}_2$  polishing slurry and improve the surface quality of polished  $\text{SiO}_2/\text{Si}_3\text{N}_4$ ,

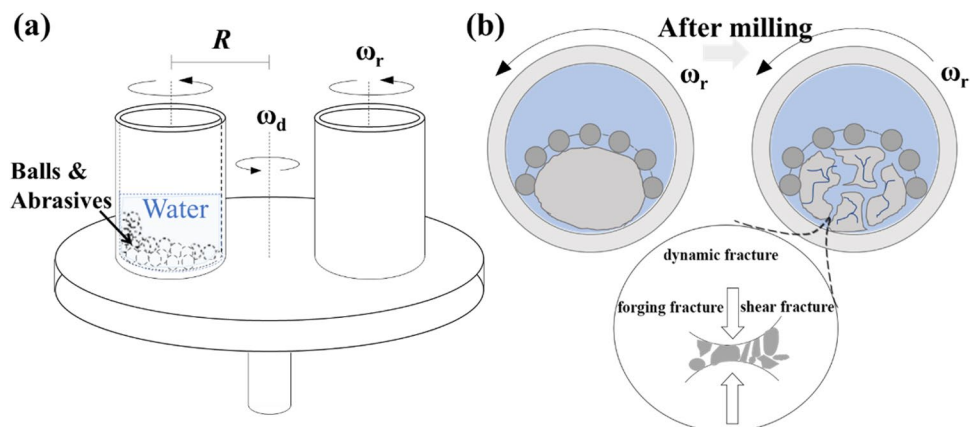
non-ionic surfactants were introduced into  $\text{CeO}_2$ -based polishing slurry. By studying the effect of non-ionic surfactants on the zeta potential of  $\text{CeO}_2$  particles, the mechanism of action is explained in more detail and objectively. In addition, the effect of pH value on the removal selectivity of  $\text{SiO}_2$  and  $\text{Si}_3\text{N}_4$  provides a reference for subsequent research on polishing liquid systems.

Here, attention is given to researching the STI CMP process by introducing various non-ionic surfactants into  $\text{CeO}_2$ -based slurries, aiming to control MRRs, removal selectivity, and surface qualities after CMP process. Five types of non-ionic surfactants were compared, and the two superior surfactants for better dispersion of  $\text{CeO}_2$  slurries were selected. The impact of chosen surfactants on MRRs, removal selectivity between  $\text{SiO}_2$  and  $\text{Si}_3\text{N}_4$ , and surface characteristics was next investigated by polishing trials at different pH levels. Depth of scratches on polished wafers and corresponding surface roughness, as well as morphology of  $\text{CeO}_2$  abrasive particles, were characterized utilizing atomic force microscope (AFM) and scanning electron microscope (SEM), respectively. Moreover, the action mechanisms of surfactants on  $\text{SiO}_2$  and  $\text{Si}_3\text{N}_4$  wafers were investigated thoroughly by surface adsorption tests, thermogravimetric analysis, zeta potential measurements, and chemical valence bond structure analysis, respectively.

## 2 Experimental

In Fig. 1a, the studied  $\text{CeO}_2$  slurries were prepared by ball milling  $\text{CeO}_2$  bonded abrasive mixed with five different non-ionic surfactants for 12 h according to the specific mass proportion: zirconia grinding ball with 1 mm diameter:  $\text{CeO}_2$  bonded abrasive: each kind of non-ionic surfactant: deionized water (DIW) = 5:1:1:32. When the ratio of the rotational speed of the ball milling tank to the sun disk is 2 (Fig. 1b), the grinding balls are in close contact with the grinding particles, resulting in a better grinding effect on the particles. Then

**Fig. 1** **a** Schematic diagram of ball milling method. **b** Changes in abrasive particles before and after ball milling



sedimentation experiments were performed for 0 and 7 days to evaluate the delamination outcomes in order to select the efficient surfactants with the best dispersibility and stability. The employed slurries for all CMP tests and other measurements were made by diluting the selected suspension by 100 times.

Polishing experiments were conducted on a Universal 150 Plus Polisher (Hwasting Technology) with a type of rigid polishing pad (DH3002-T80D30-S20M3S1). All wafers were polished at a slurry flow rate of 150 mL/min with platen/carrier speed of 93/87 rpm for 60 s. Prior to each experiment, pad break-in conditioning was conducted for 600 s using a diamond disk. After polishing, all wafers were rinsed with DIW and dried with nitrogen gas in sequence. The thicknesses of the polished 4-in  $\text{SiO}_2$  and  $\text{Si}_3\text{N}_4$  wafers were measured using an optical interferometer (F50, Filmetrics) at 81 different locations on each wafer surface followed by averaging. Each experiment was repeated at least thrice, and the obtained data were used to calculate the average material removal rates and standard deviations.

The morphology of modified  $\text{CeO}_2$  abrasive particles by non-ionic surfactants was carried out by scanning electron microscope (SU8220, Hitachi) at a voltage of 5 kV. Zeta potentials and particle sizes of the modified slurries were measured using a laser particle size analyzer (Nano-ZS90, Malvern Instrument), where the transparent samples were prepared by diluting (3.125 wt.%) and sonicating of the selected suspension for 300 s (KUDOS) and then vibrating at a speed of 1600 r/min for 300 s in a thermal vortex mixer. For the zeta potential measurement of wafer surfaces, a solid surface zeta analyzer (SurPASS<sup>TM</sup> 3, Anton Paar) was used. Moreover, thermogravimetric analysis (TGA) of the prepared  $\text{CeO}_2$  slurries were performed using a platinum crucible with nitrogen at 0–750 °C. A rotating rheometer (Anton Paar Physica MCR302) was employed to test the rheological properties of the modified  $\text{CeO}_2$  slurries. Quartz crystal microbalance (Q-sense, Sweden Biolin Scientific) was used to characterize and analyze the adsorption properties of solid–liquid interface adsorption between the modified  $\text{CeO}_2$  slurries and  $\text{SiO}_2/\text{Si}_3\text{N}_4$  surfaces. What's more, an atomic force microscope (Dimension ICON of Bruker) was utilized to map surface conditions of polished  $\text{SiO}_2$  and  $\text{Si}_3\text{N}_4$  wafers, where the obtained AFM images were scanned at a rate of 1 Hz on a surface area of  $5 \times 5 \mu\text{m}$  for all wafers.

### 3 Results and discussion

#### 3.1 Preparation and selection of $\text{CeO}_2$ slurries with various non-ionic surfactants

To modify and improve the polishing slurries for STI CMP process, various polymers as non-ionic surfactants which have different functional groups were introduced in the

**Table 1** Symbols and abbreviations of proper noun

Full name	abbreviation
Chemical mechanical polishing	CMP
Shallow trench isolation	STI
Ceria	$\text{CeO}_2$
Silicon dioxide	$\text{SiO}_2$
Silicon nitride	$\text{Si}_3\text{N}_4$
Material removal rate	MRR
Atomic force microscope	AFM
Scanning electron microscope	SEM
Deionized water	DIW
Thermogravimetric analysis	TGA
Polyethylpyrrolidone	PVP-K30
Polyethylene glycol	PEG
Polyacrylamide	PAM
Polyvinyl alcohol	PVA-124
Polypropylene glycol	PPG
Frequency	$\Delta f$
Dissipation	$\Delta D$
The adsorption mass change	$\Delta m$

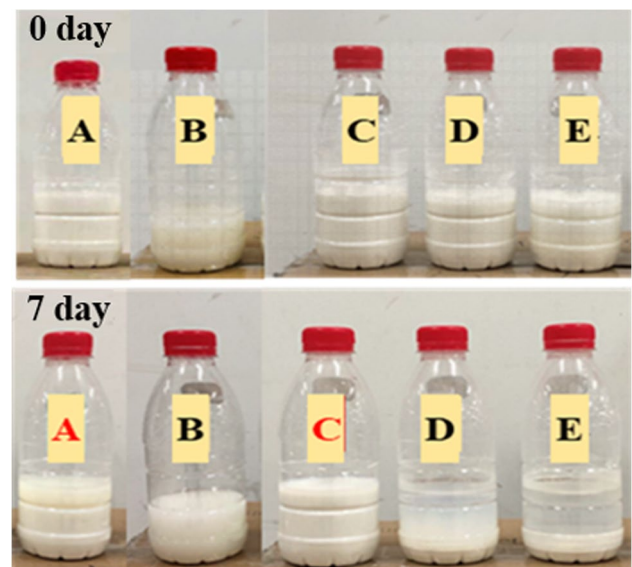


**Fig. 2** Comparison test of  $\text{CeO}_2$  bonded abrasive with different non-ionic surfactants after ball milling and subsiding for 0 and 7 days

preparation process of  $\text{CeO}_2$  slurries, involving polyethylene glycol (PEG, sample A), polyacrylamide (PAM, sample B), polyethylpyrrolidone (PVP-K30, sample C), polyvinyl alcohol (PVA-124, sample D), and polypropylene glycol (PPG, sample E). We give the symbols and abbreviations of all proper noun in Table 1. The settling results of  $\text{CeO}_2$  bonded abrasives mixed with these non-ionic surfactants after 0 and 7 days of standing are shown in Fig. 2. It should

be emphasized that the presence of additional sediments and clear stratification results in poor dispersibility and stability for polishing slurries. It is apparent that the stability of  $\text{CeO}_2$  slurries was excellent following the addition of surfactants C and A, which are PVP-K30 and PEG, respectively, while all of the  $\text{CeO}_2$  slurries mixed with the other three surfactants displayed noticeable sedimentation.

The dispersion effects of PVP-K30 and PEG on  $\text{CeO}_2$  particles were further compared, where the two mixed suspensions and the control group without any additive were naturally dried at room temperature to observe the particle morphology. As shown in Fig. 3a, after the addition of PVP-K30, it can be observed that the diameter of a single  $\text{CeO}_2$  abrasive particle was approximately 60 nm. Meanwhile, there was a significant separation between each individual abrasive particle, indicating an excellent dispersion of  $\text{CeO}_2$  slurries. Figure 3b presents the effect of PEG on  $\text{CeO}_2$  particles, where the diameter of each single abrasive particle

was around 60~150 nm. Although a portion of  $\text{CeO}_2$  particles was aggregated owing to the capillary force, the dispersion of the  $\text{CeO}_2$  slurries was still improved. In contrast, the  $\text{CeO}_2$  suspensions without any addition of surfactants were mapped in Fig. 3c. The diameter of  $\text{CeO}_2$  particles was about 120~150 nm with a phenomenon of agglomeration. As shown, the addition of PVP-K30 and PEG is capable of enhancing the dispersion of  $\text{CeO}_2$  abrasive particles.

The distinct dispersion effect of PVP-K30 and PEG on  $\text{CeO}_2$  can be attributed to their structural differences. The functional group of  $\text{C}=\text{O}$  in PVP monomer could form hydrogen bonds with  $\text{CeO}_2$  and finally form the  $\text{CeO}_2$ -PVP- $\text{CeO}_2$  structure, which could produce a good dispersion effect on  $\text{CeO}_2$ , as shown in Fig. 4a. This structure was proposed in the  $\text{CeO}_2$ - $\text{SiO}_2$  composite particles synthesized by Lu et al. [13] to disperse and connect  $\text{CeO}_2$  and  $\text{SiO}_2$  particles uniformly. Moreover, the oxygen atoms of the  $\text{C}-\text{O}$  bond in PEG and the oxygen atoms in

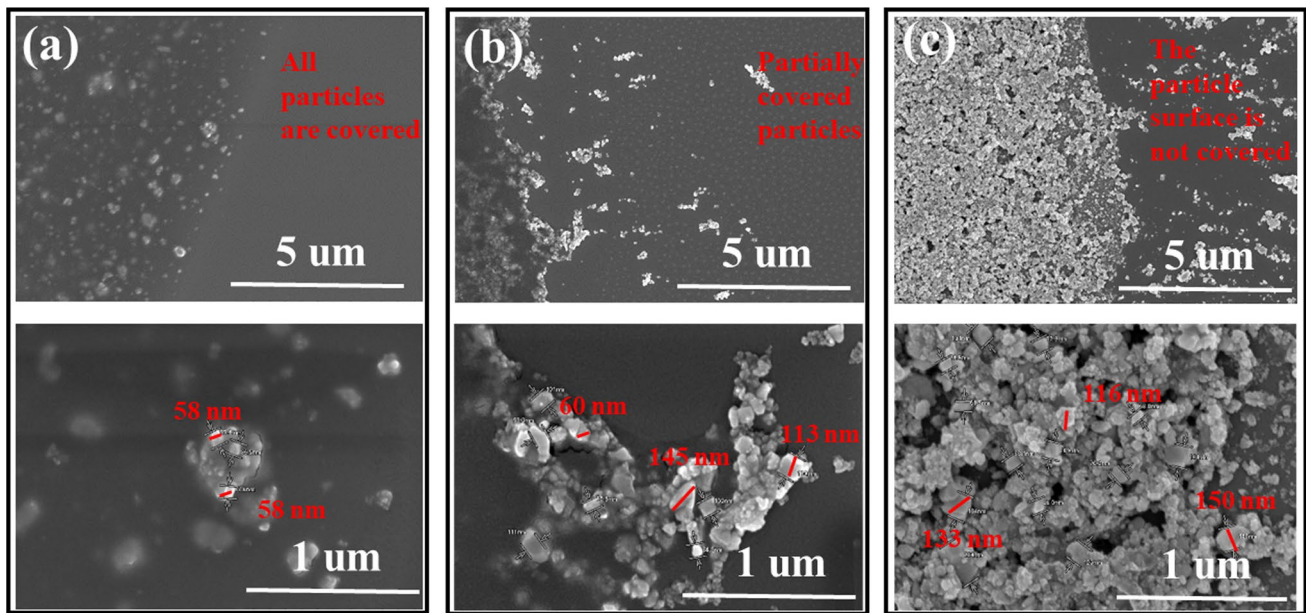


**Fig. 3** SEM morphology of  $\text{CeO}_2$  abrasive particles **a** with PVP-K30 added, **b** with PEG added, and **c** without any surfactant added after natural air drying

**Fig. 4** Dispersion mechanism diagram of **a** PVP-K30 and **b** PEG with  $\text{CeO}_2$

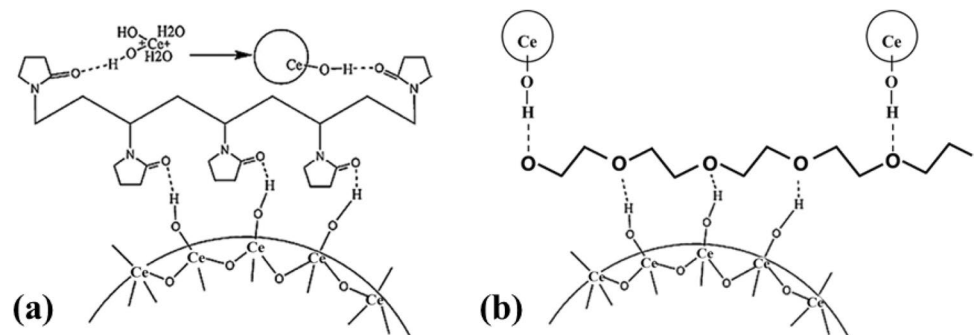
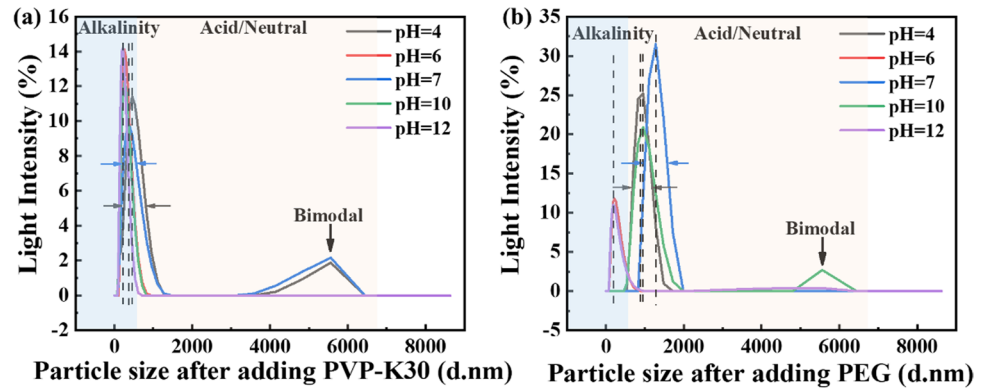




**Fig. 5** Particle size distribution of  $\text{CeO}_2$  slurries with the treatment of **a** PVP-K30 and **b** PEG at different pH values



$\text{CeO}_2$  can be connected by hydrogen bonds, resulting in a  $\text{CeO}_2$ -PEG- $\text{CeO}_2$  structure, which could provide a good dispersion effect too (Fig. 4b). In particular, the oxygen atoms in PEG are separated by C-O and C-C bonds, while oxygen atoms in PVP are only separated by C-C bonds. The more C-O bonds of PEG than PVP-K30 make the folding effect of PEG more significant than that of PVP-K30 when forming hydrogen bonds with oxygen atoms of the same distance on  $\text{CeO}_2$  particle surfaces, which makes the dispersion effect of PEG less than that of PVP-K30.

### 3.2 Stability of $\text{CeO}_2$ slurries with PVP-K30/PEG at different pH values

To further figure out the stability of  $\text{CeO}_2$  slurries with PVP-K30 and PEG, particle size distribution of  $\text{CeO}_2$  particles was compared at different pH values, as illustrated in Fig. 5. Quite similar tendency emerged with the addition of these two non-ionic surfactants that the half-peak width of  $\text{CeO}_2$  particle size distribution in acidic and neutral environments is significantly larger than that in alkaline condition, indicating a more stable and uniform particle condition in high pH levels. Meanwhile, an interesting bimodal phenomenon both appeared under the action of PVP-K30 and PEG, where the pH levels for their occurrence are quite different.

Figure 6 depicts the specific particle sizes of  $\text{CeO}_2$  abrasive at different pH values after the addition of PVP-K30 and PEG. The findings demonstrate that these two surfactants have a downward impact on  $\text{CeO}_2$  abrasive particle sizes. Specifically, at pH values of 4, 6, 7, 10, and 12, the Z-average particle sizes of  $\text{CeO}_2$  abrasive particle with PVP-K30 had a reduction of 77, 69, 84, 74, and 20%, while that with PEG decreased by 45, 75, 19, and 24%, respectively.

### 3.3 Effect of $\text{CeO}_2$ slurries with PVP-K30 and PEG on CMP process

The MRRs of  $\text{Si}_3\text{N}_4$  in  $\text{CeO}_2$ -based slurries with the addition of PVP-K30 and PEG at different pH levels are depicted

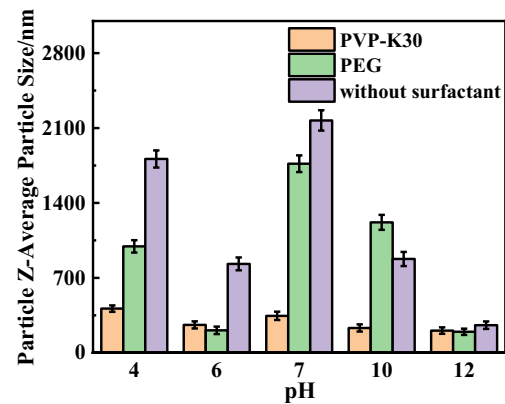


**Fig. 6** Average particle sizes of  $\text{CeO}_2$  with/without the addition of PVP-K30 and PEG at different pH values

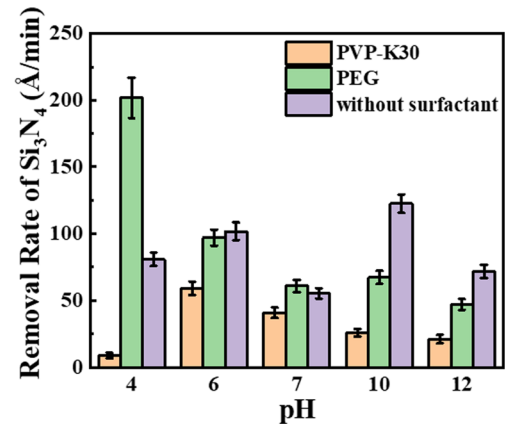


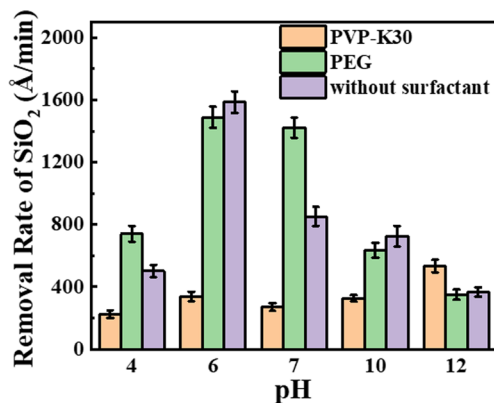
**Fig. 7** MRRs of  $\text{Si}_3\text{N}_4$  polished by  $\text{CeO}_2$  slurries with/without the addition of PVP-K30 and PEG at different pH values

in Fig. 7. At pH values of 4, 6, 7, 10, and 12, the MRRs of  $\text{Si}_3\text{N}_4$  polished by  $\text{CeO}_2$  slurries with PVP-K30 were 9, 59, 41, 26, and 21  $\text{\AA}/\text{min}$ , respectively, achieving the goal for  $\text{Si}_3\text{N}_4$  MRR of less than 50  $\text{\AA}/\text{min}$ . Compared with polished without any surfactant, the maximum  $\text{Si}_3\text{N}_4$  MRR inhibition

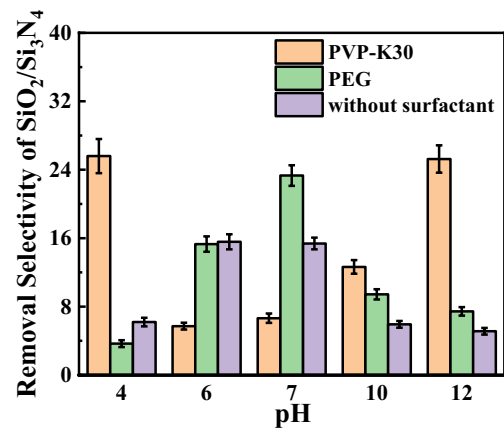
of 89% could be achieved by the addition of PVP-K30 at pH 4. On the other hand, the MRRs of  $\text{Si}_3\text{N}_4$  after polished by PEG in  $\text{CeO}_2$  slurries were 202, 97, 61, 67, and 47 Å/min at different five pH values, respectively. It can be observed that at pH values of 4 and 7, PEG presents no inhibition impact on  $\text{Si}_3\text{N}_4$  removal rates, whereas the MRRs of  $\text{Si}_3\text{N}_4$  with PEG had a reduction of 5, 45, and 35% at pH values of 6, 10, and 12. By comparison, it was found that the inhibition of PVP-K30 on  $\text{Si}_3\text{N}_4$  removal is stronger than that by PEG at all pH conditions.

Figure 8 presents the effect of PVP-K30 and PEG on  $\text{SiO}_2$  MRRs in  $\text{CeO}_2$ -based slurries. When pH values were 4, 6, 7, and 10, the MRRs of  $\text{SiO}_2$  polished by  $\text{CeO}_2$  slurries with PVP-K30 were 226, 339, 271, and 327 Å/min, respectively. Compared with the polishing results without any surfactant,  $\text{SiO}_2$  MRRs were inhibited by PVP-K30 with a reduction of 55, 79, 68, and 55%. However, the  $\text{SiO}_2$  MRR (534 Å/min) with the addition of PVP-K30 was higher than that without any surfactant (368 Å/min) at pH 12. On the other hand, at five different pH conditions, the removal rates of  $\text{SiO}_2$  after polished by  $\text{CeO}_2$  slurries with PEG were 741, 1489, 1422, 635, and 350 Å/min, fluctuating considerably. At pH values of 6, 10, and 12, PEG inhibited  $\text{SiO}_2$  MRRs slightly, which decreased by 6, 12, and 5%, respectively. As a result, it can be concluded that PVP-K30 could present a stronger inhibition on  $\text{SiO}_2$  MRRs than PEG at pH values of 4, 6, 7, and 10.

Figure 9 shows the removal selectivity between  $\text{SiO}_2$  and  $\text{Si}_3\text{N}_4$  at different pH values polished using  $\text{CeO}_2$  slurries with PVP-K30 and PEG added. At pH 4, 10, and 12, the removal selection ratios ( $\sim 26$ ,  $\sim 13$ , and  $\sim 25$ ) between  $\text{SiO}_2$  and  $\text{Si}_3\text{N}_4$  polished by  $\text{CeO}_2$  slurries with PVP-K30 were higher than those polished by slurries with PEG or without any surfactant addition, while with the addition of PEG, greater removal selection ratio could be achieved at pH 7. This demonstrates that PVP-K30 could play a role on removal selectivity at acidic and alkaline regions, whereas



**Fig. 8** MRRs of  $\text{SiO}_2$  polished by  $\text{CeO}_2$  slurries with/without the addition of PVP-K30 and PEG at different pH values



**Fig. 9** Removal selectivity between  $\text{SiO}_2$  and  $\text{Si}_3\text{N}_4$  after polished by  $\text{CeO}_2$  slurries with/without the addition of PVP-K30 and PEG at different pH values

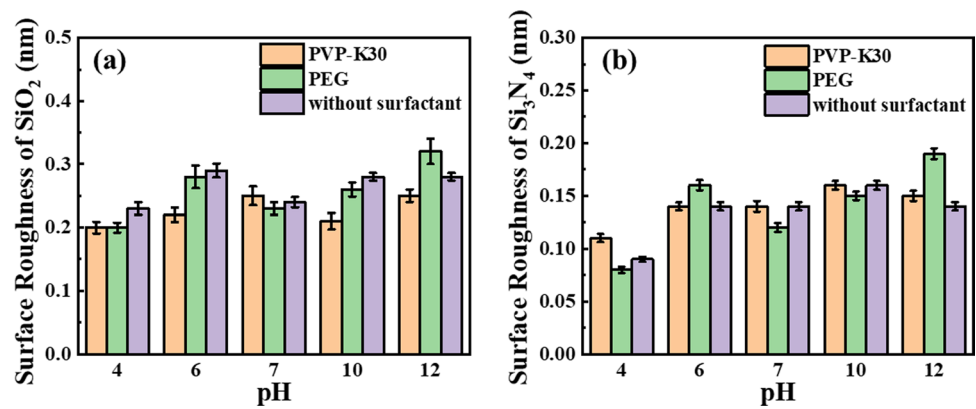
PEG has the remarkable effect when the pH environment is neutral.

Figure 10 displays the surface roughness of  $\text{SiO}_2$  and  $\text{Si}_3\text{N}_4$  after polished by  $\text{CeO}_2$  slurries with the addition of PVP-K30 or PEG at different pH levels. Although it seems that two non-ionic surfactants has little improvement on polished surface qualities, both of them meet the high demands ( $R_a < 1$  nm), where the surface roughness of  $\text{SiO}_2$  polished by  $\text{CeO}_2$  slurries with PVP-K30 or PEG added was maintained at  $0.20 \sim 0.32$  nm, and that of  $\text{Si}_3\text{N}_4$  was around  $0.08 \sim 0.16$  nm, respectively.

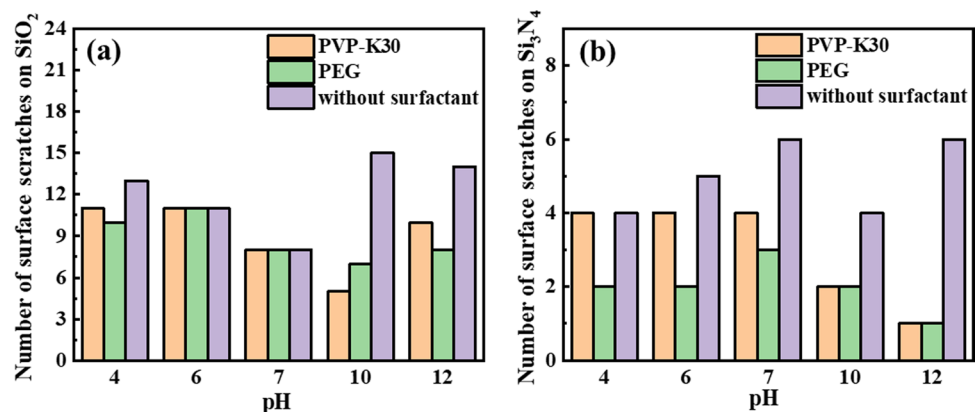
By characterizing the quantity and maximum depth of surface scratches, defects of polished  $\text{SiO}_2$  and  $\text{Si}_3\text{N}_4$  were identified. As presented in Fig. 11, the number of scratches in the range of  $5 \times 5 \mu\text{m}^2$  on the  $\text{SiO}_2$  and  $\text{Si}_3\text{N}_4$  surfaces polished by  $\text{CeO}_2$  slurries with added PVP-K30 and PEG was counted at various pH values. It was found that the number of scratches on polished  $\text{SiO}_2$  surfaces decreased after the addition of PVP-K30 and PEG compared to that without any addition of surfactants, along with a same outcome of polished  $\text{Si}_3\text{N}_4$  surfaces. Furthermore, the number of scratches on  $\text{SiO}_2$  and  $\text{Si}_3\text{N}_4$  surfaces is less in an alkaline environment than that in an acidic region.

Figures 12 and 13 show AFM images of  $\text{SiO}_2$  wafers polished by  $\text{CeO}_2$  slurries with PVP-K30 and PEG added under acidic, neutral, and alkaline environments, that is, pH values of 4, 7, and 10. The scratch depth of  $\text{SiO}_2$  wafers polished by  $\text{CeO}_2$  slurries with PVP-K30 in order from large to small is as follows: alkaline ( $\sim 700$  pm) > acidic ( $\sim 500$  pm) > neutral ( $\sim 450$  pm). However, quite different results were obtained when PEG was added in  $\text{CeO}_2$  slurries, where the maximum scratch depth of  $\sim 700$  pm occurred in neutral environment, whereas the slightest scratch depth was  $\sim 400$  pm in acidic region. Similarly, Figs. 14 and 15 show the surface morphology of polished  $\text{Si}_3\text{N}_4$  with the mixed slurries at pH

**Fig. 10** Surface roughness of **a**  $\text{SiO}_2$  and **b**  $\text{Si}_3\text{N}_4$  after polished by  $\text{CeO}_2$  slurries with/without the addition of PVP-K30 and PEG at different pH values



**Fig. 11** Number of surface scratches on **a**  $\text{SiO}_2$  and **b**  $\text{Si}_3\text{N}_4$  after polished by  $\text{CeO}_2$  slurries with/without PVP-K30 and PEG at different pH values



values of 4, 7, and 10. After polished by PVP-K30, the largest scratch depth on  $\text{Si}_3\text{N}_4$  surfaces occurred in acidic condition of  $\sim 450$  pm, followed by neutral and basic environment of  $\sim 400$  pm. After polished by PEG, the maximum scratch depth of  $\text{Si}_3\text{N}_4$  surfaces can be found in alkaline condition ( $\sim 450$  pm), followed by neutral ( $\sim 350$  pm), and then acid environment ( $\sim 300$  pm). In general, the maximum scratch depth of polished  $\text{SiO}_2$  surfaces was greater than that of  $\text{Si}_3\text{N}_4$  surfaces at the same pH condition. Owing to the presence of mechanical action during material removal,  $\text{SiO}_2$  has a higher removal rate than  $\text{Si}_3\text{N}_4$ , accompanied by greater surface wear than  $\text{Si}_3\text{N}_4$ , and thus a greater maximum surface scratch depth for  $\text{SiO}_2$ .

### 3.4 Adsorption behavior of PVP-K30 and PEG on $\text{SiO}_2$ and $\text{Si}_3\text{N}_4$ surfaces

There is a uniform rule at pH values of 4, 6, 7, and 10 that PVP-K30 has a greater inhibitory effect on the removal of  $\text{SiO}_2$  and  $\text{Si}_3\text{N}_4$  than PEG. The two mixed suspensions were selected at pH value of 4 to analyze their adsorption on the surfaces of  $\text{SiO}_2$  and  $\text{Si}_3\text{N}_4$ . A quartz crystal microbalance was used as a characterization instrument, DIW was injected into  $\text{SiO}_2$  (or  $\text{Si}_3\text{N}_4$ ) as the base solution, and baseline frequency signals were measured after stabilization. When  $\text{CeO}_2$

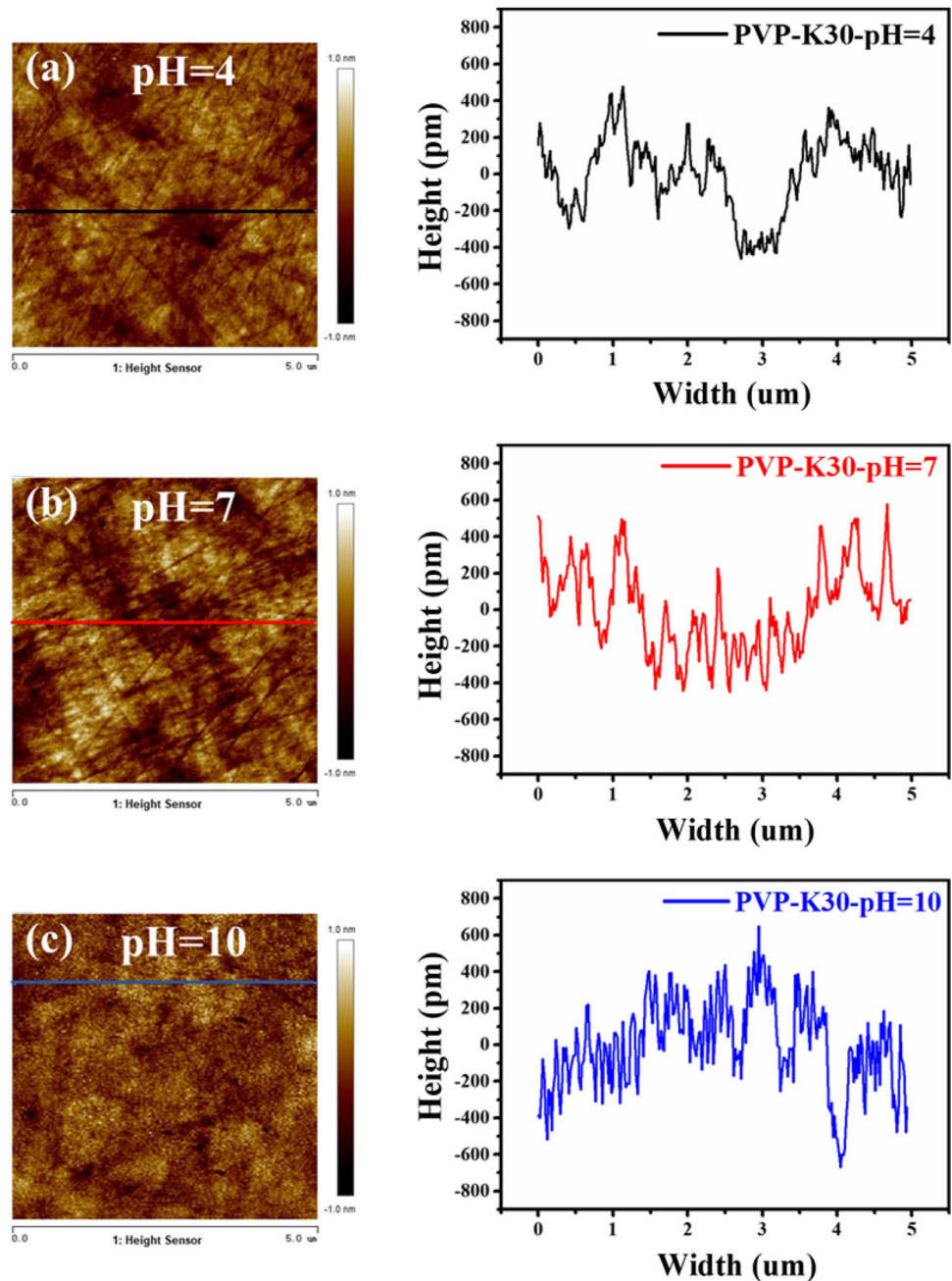
slurries containing PVP-K30 or PEG were injected into  $\text{SiO}_2$  (or  $\text{Si}_3\text{N}_4$ ) chips at a flow rate of 0.2 mL/min, the vibration frequency of  $\text{SiO}_2$  (or  $\text{Si}_3\text{N}_4$ ) changed. Simultaneously, the frequency reduction of the third overtone and the dissipation caused by adsorption at 25 °C were recorded. When the adsorption amount gradually increased to a stable value, the vibration frequency and surface dissipation of  $\text{SiO}_2$  (or  $\text{Si}_3\text{N}_4$ ) tended to stabilize. The vibration frequency of the stabilized  $\text{SiO}_2$  (or  $\text{Si}_3\text{N}_4$ ) after passing through  $\text{CeO}_2$  slurries containing PVP-K30 or PEG solution was compared with the vibration frequency of  $\text{SiO}_2$  (or  $\text{Si}_3\text{N}_4$ ) when passing through DIW, and the difference was taken as the resonance frequency ( $\Delta f$ ) of the adsorption of PVP-K30 and PEG molecules on  $\text{SiO}_2$  and  $\text{Si}_3\text{N}_4$ . Similarly, the change in the surface dissipation ( $\Delta D$ ) of  $\text{SiO}_2$  and  $\text{Si}_3\text{N}_4$  was calculated.

When the dissipation is sufficiently small ( $\Delta D < 10|\Delta f|$ ), the adsorption film is rigid and has low viscoelasticity. According to Eq. (1), the frequency change can be converted into the adsorption mass change ( $\Delta m$ ) using the Sauerbrey equation [14]:

$$\Delta m = -C \frac{\Delta f}{n} \quad (1)$$

where  $C$  is a constant ( $17.7 \text{ ng} \cdot \text{Hz}^{-1} \cdot \text{cm}^{-2}$ ) related to the properties of the quartz crystal and  $n$  is the overtone

**Fig. 12** Surface morphology of  $\text{SiO}_2$  polished by  $\text{CeO}_2$  slurries with PVP-K30 added at **a** pH 4, **b** pH 7, and **c** pH 10



of oscillation (3 for  $\text{SiO}_2$  and  $\text{Si}_3\text{N}_4$  wafers with 150 mm diameter).

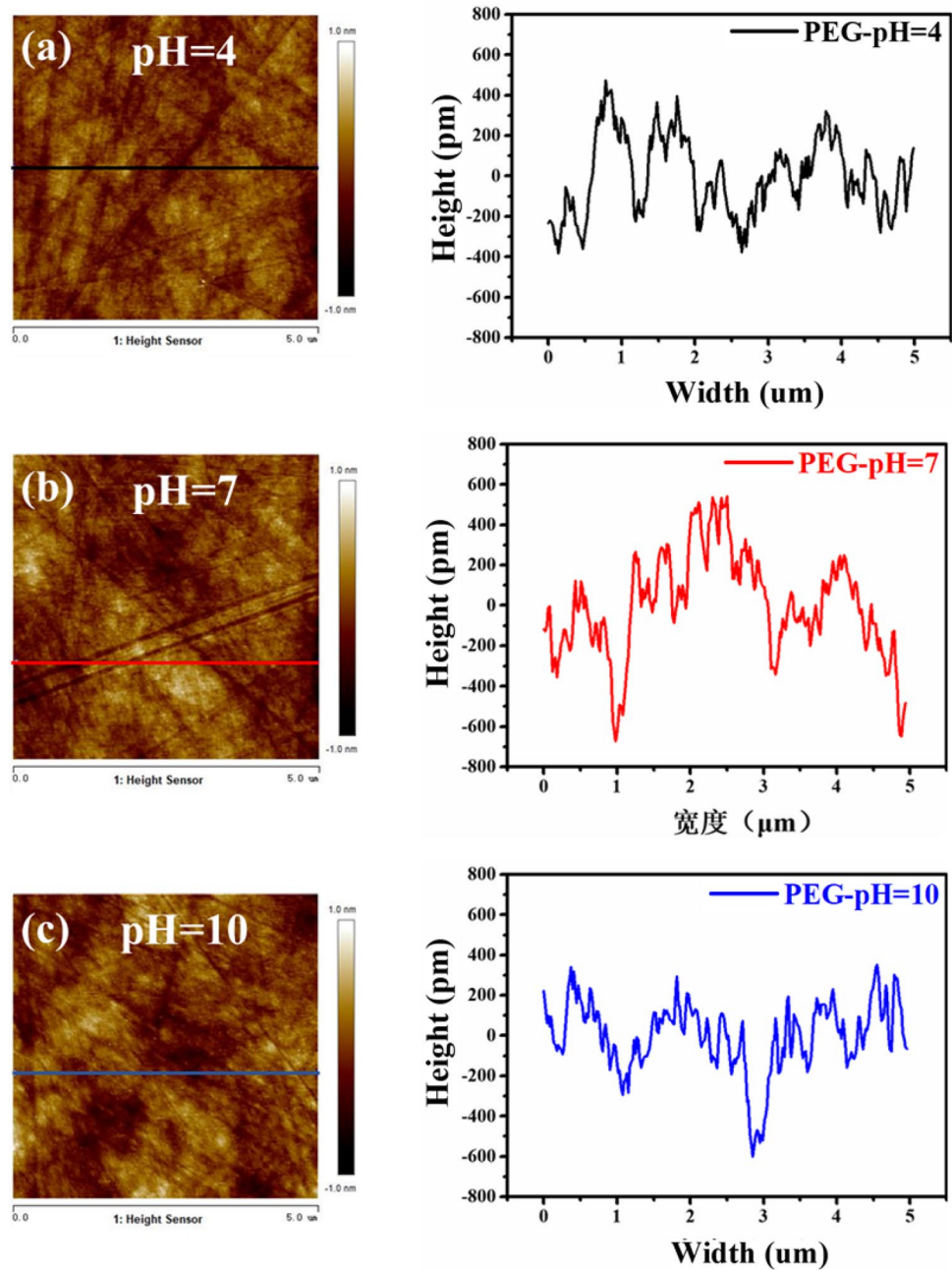
As shown in Fig. 16, when the adsorption amount of PVP-K30 on the  $\text{SiO}_2$  surface gradually became stable, the resonance frequency of PVP-K30 molecular adsorption on  $\text{SiO}_2$  was approximately 23 Hz, and the change in surface dissipation was approximately 3 ppm. As shown in Fig. 17, when the adsorption amount of PEG on the  $\text{SiO}_2$  surface gradually stabilized, the  $\Delta f$  of PEG molecule adsorption on  $\text{SiO}_2$  was approximately 10 Hz with a  $\Delta D$  approximately of 1.2 ppm. In both cases, the dissipations are sufficiently small ( $\Delta D < 10|\Delta f|$ ), indicating that the adsorption films of

PVP-K30 and PEG on  $\text{SiO}_2$  surfaces are rigid and have low viscoelasticity. The adsorption mass on the  $\text{SiO}_2$  surface ( $\Delta m$ ) can be calculated using Eq. (1) as 240 ng and 104 ng, respectively.

The adsorption behavior of PVP-K30 and PEG on  $\text{Si}_3\text{N}_4$  wafers was identified using the same approach, as depicted in Figs. 18 and 19. The same conclusions can be drawn that the adsorption films of PVP-K30 and PEG on  $\text{Si}_3\text{N}_4$  surfaces are rigid with low viscoelasticity and have an adsorption mass of around 198 and 73 ng, respectively. It was found that the adsorption mass of PVP-K30 on  $\text{SiO}_2$  and  $\text{Si}_3\text{N}_4$  surfaces was greater than that of PEG, which could explain



**Fig. 13** Surface morphology of  $\text{SiO}_2$  polished by  $\text{CeO}_2$  slurries with PEG added at **a** pH 4, **b** pH 7, and **c** pH 10



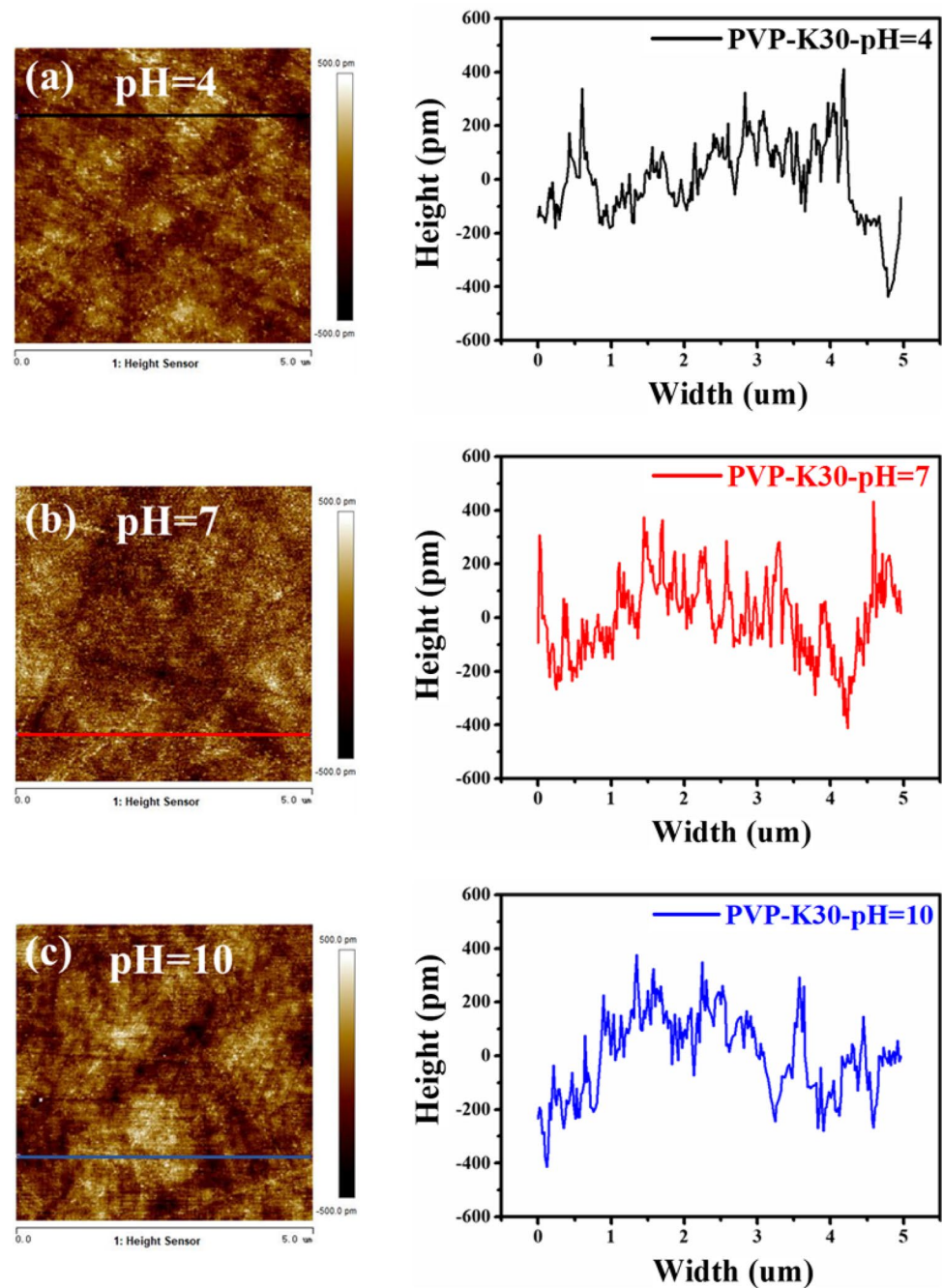
why when the pH value was 4, PVP-K30 had a stronger inhibitory effect on the removal of  $\text{SiO}_2$  and  $\text{Si}_3\text{N}_4$  than that of PEG.

### 3.5 Adsorption behavior of PVP-K30 and PEG on $\text{CeO}_2$ particles

When the pH values are 4, 6, 7, and 10, PVP-K30 has a greater inhibition on the removal of  $\text{SiO}_2$  and  $\text{Si}_3\text{N}_4$  than that of PEG. At a pH value of 6, the two mixed slurries were subjected to thermogravimetric analysis. It is known that the boiling point of PEG is greater than  $250^\circ\text{C}$  and

that of PVP-K30 is greater than  $350^\circ\text{C}$ . In Fig. 20, with an increasing temperature, the two mixed slurries lose weight gradually at first and then begin to lose weight rapidly when the temperature is close to  $100^\circ\text{C}$ . This stage is a part of the water evaporation process. The weight loss beyond  $100^\circ\text{C}$  is the decomposition stage of the remaining solid substances at high temperatures. The mass of the mixture of PEG and  $\text{CeO}_2$  remained unchanged from  $100$  to  $250^\circ\text{C}$  after the first stage of rapid weight loss ( $0$  to  $100^\circ\text{C}$ ). It underwent weight loss in the second stage at  $250^\circ\text{C}$ , and its mass did not change beyond approximately  $380^\circ\text{C}$ . The mixture of PVP-K30 and  $\text{CeO}_2$  experienced rapid weight loss in the

**Fig. 14** Surface morphology of  $\text{Si}_3\text{N}_4$  polished by  $\text{CeO}_2$  slurries with PVP-K30 added at **a** pH 4, **b** pH 7, and **c** pH 10



first stage (0–100 °C) and its mass remained unchanged at approximately 100–350 °C. It experienced weight loss at 350 °C from the second stage, and its mass did not change beyond approximately 500 °C. After adding PEG and PVP-K30, the weight loss temperature in the second stage was consistent with the boiling points of PEG and PVP-K30. This indicates that PEG and PVP-K30 are still adsorbed on the abrasive surface during water evaporation. When DIW is completely evaporated, it needs to be heated to the boiling point of PEG and PVP-K30 before they leave the abrasive surface.

### 3.6 Zeta potential analysis of $\text{SiO}_2$ and $\text{CeO}_2$ slurries with PVP-K30 and PEG

To further explore the removal mechanisms, zeta potentials of  $\text{CeO}_2$  mixed slurries with PVP-K30 and PEG added were analyzed at different pH values, as shown in Fig. 21. After adding PEG and PVP-K30, the surface zeta potentials are positive at pH values of 4 and 6, indicating that there is a gravitational interaction between  $\text{CeO}_2$  abrasive particles and  $\text{SiO}_2$  surfaces. The absolute value of the zeta potential of PVP-K30 and  $\text{CeO}_2$  mixed suspension is less than that of

**Fig. 15** Surface morphology of  $\text{Si}_3\text{N}_4$  polished by  $\text{CeO}_2$  slurries with PEG added at **a** pH 4, **b** pH 7, and **c** pH 10

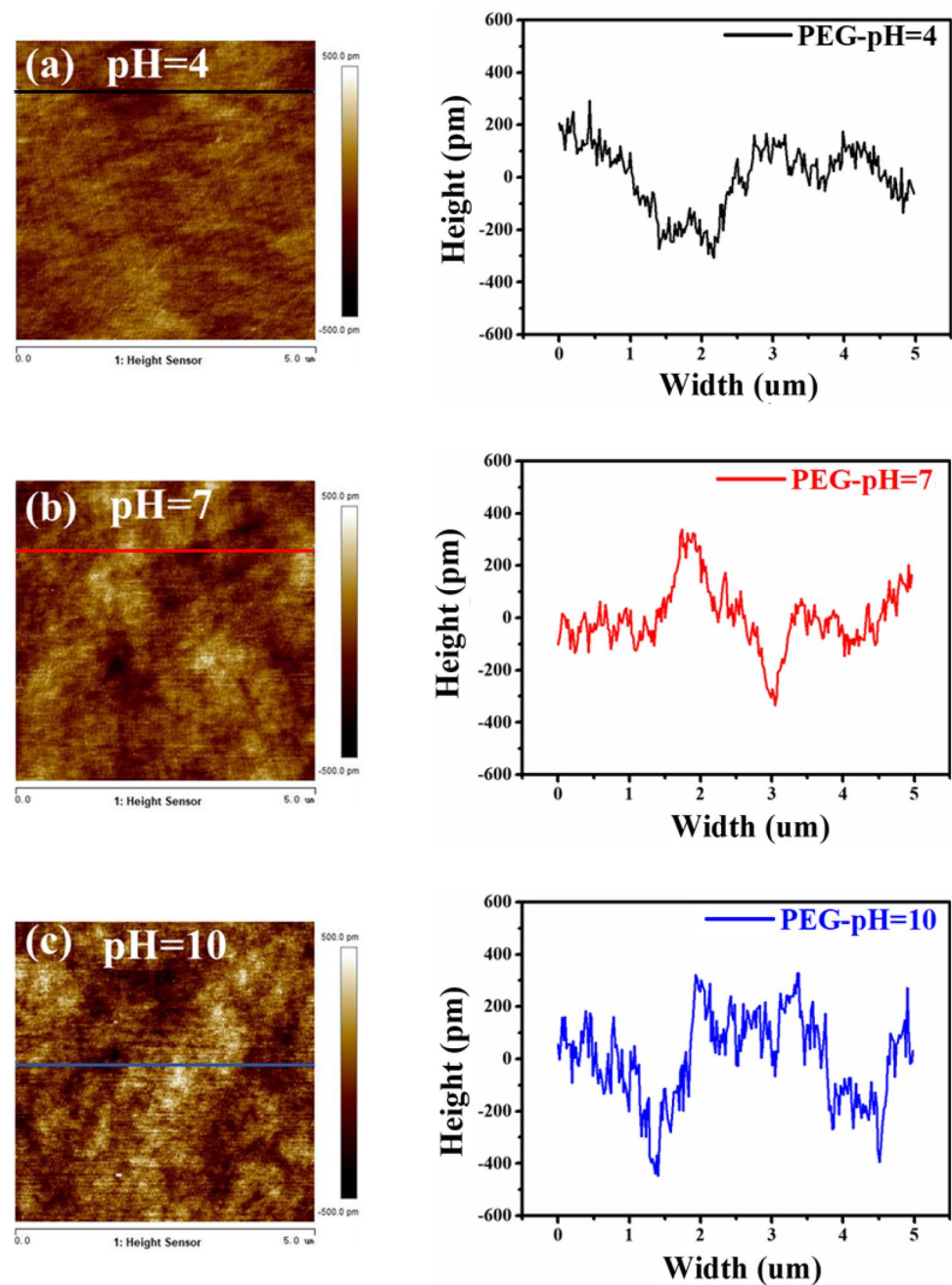


**Fig. 16** **a** Vibration frequency and **b** surface dissipation of PVP-K30 in  $\text{CeO}_2$  slurries on  $\text{SiO}_2$  surfaces at pH 4

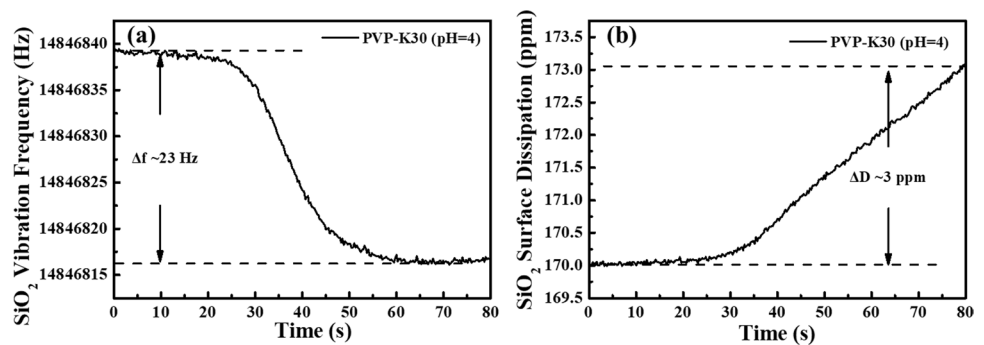


**Fig. 17** **a** Vibration frequency and **b** surface dissipation of PEG in  $\text{CeO}_2$  slurries on  $\text{SiO}_2$  surfaces at pH 4

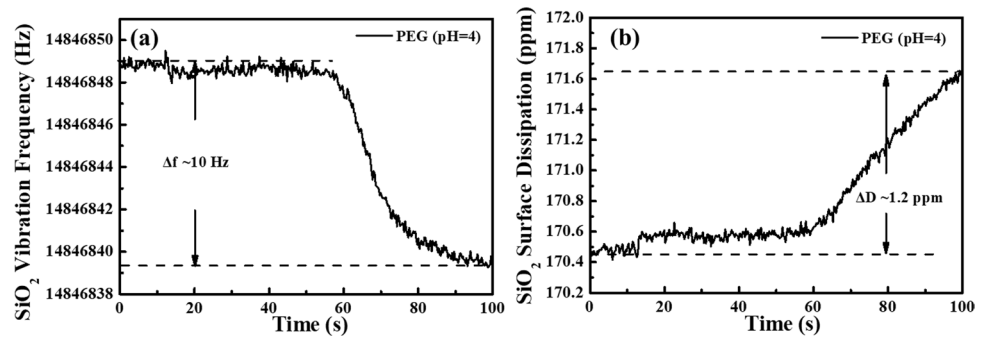


**Fig. 18** **a** Vibration frequency and **b** surface dissipation of PVP-K30 in  $\text{CeO}_2$  slurries on  $\text{Si}_3\text{N}_4$  surfaces at pH 4

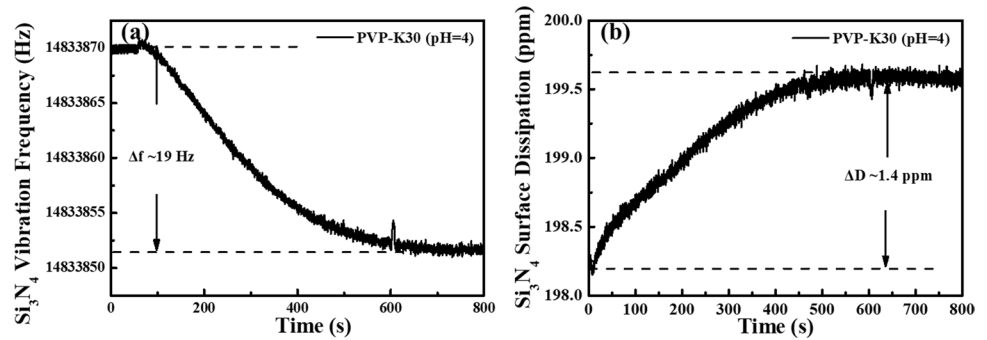


**Fig. 19** **a** Vibration frequency and **b** surface dissipation of PEG in  $\text{CeO}_2$  slurries on  $\text{Si}_3\text{N}_4$  surfaces at pH 4

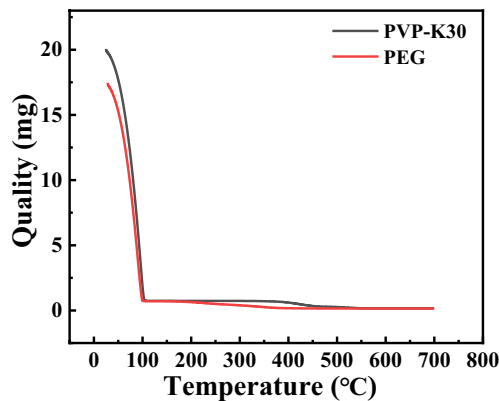
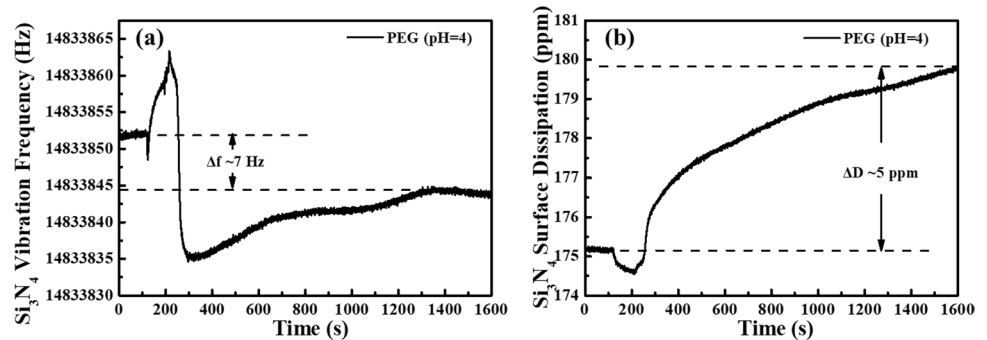


**Fig. 20** TGA analysis curves of  $\text{CeO}_2$  mixed slurries with PVP-K30 and PEG

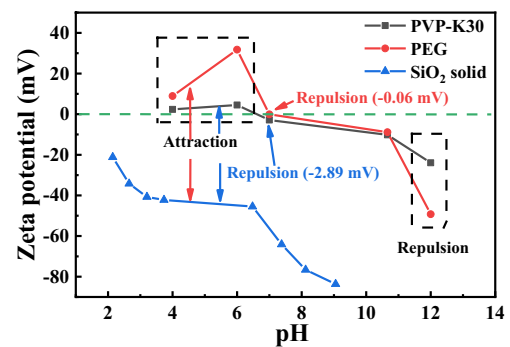


**Fig. 21** Zeta potentials of  $\text{CeO}_2$  mixed slurries with **a** PVP-K30 and **b** PEG and **c**  $\text{SiO}_2$  solid surface at different pH values



PEG and  $\text{CeO}_2$  mixed one; this shows that the gravity of the former and  $\text{SiO}_2$  is less than that of the latter. This further explains why PVP-K30 has stronger removal inhibition on  $\text{SiO}_2$  than PEG at pH values of 4 and 6. The surface zeta potentials of the two mixed suspensions are negative at pH values of 7, 10, and 12, and there will be a repulsive force between  $\text{CeO}_2$  abrasive particles and  $\text{SiO}_2$  surfaces. When pH values are 7 and 10, the absolute value of zeta potentials of PVP-K30 and  $\text{CeO}_2$  mixed suspension is greater than that of PEG and  $\text{CeO}_2$  mixed one, which proves that the repulsion between the former and  $\text{SiO}_2$  is greater than that of the latter. When the pH value is 12, the absolute value of zeta potential of the  $\text{CeO}_2$  mixed slurry with PVP-K30 added is smaller than that of the  $\text{CeO}_2$  mixed slurry with added PEG, which proves that the repulsion between the former and  $\text{SiO}_2$  is smaller than that of the latter. This further explains why PVP-K30 has stronger removal inhibition on  $\text{SiO}_2$  than PEG at pH values of 7 and 10. The removal rate of  $\text{SiO}_2$  after adding PEG is lower than that after adding PVP-K30 when the pH value is 12.

Here, the dispersion effects of various non-ionic surfactants on  $\text{CeO}_2$  particles were compared. It was found that PVP-K30 and PEG can uniformly disperse  $\text{CeO}_2$  particles and achieve suitable removal selectivity between  $\text{SiO}_2$  and  $\text{Si}_3\text{N}_4$ . We focused on the effect of  $\text{CeO}_2$  polishing slurry containing non-ionic surfactants on the surface quality of polished  $\text{SiO}_2$  and  $\text{Si}_3\text{N}_4$  wafers. In addition, the effect of pH value on the selectivity of  $\text{SiO}_2$  and  $\text{Si}_3\text{N}_4$  removal provides a reference for subsequent research on polishing slurry systems.

## 4 Conclusions

In this study, the influence mechanism of the non-ionic surfactants PVP-K30 and PEG on the dispersion of  $\text{CeO}_2$  slurries and the removal of  $\text{SiO}_2$  and  $\text{Si}_3\text{N}_4$  were investigated. The following conclusions were drawn from the study:

(1) Non-ionic surfactants can be adsorbed on  $\text{CeO}_2$  abrasive particles by forming hydrogen bonds, where the adsorption mode is slightly affected by pH values. The Z-average particle sizes of  $\text{CeO}_2$  suspensions were 200–400 nm at different pH values after the addition of PVP-K30.

(2) Among various non-ionic surfactants, PVP-K30 has a stronger dispersion effect on  $\text{CeO}_2$  particles than PEG since PEG has more C–O bonds than PVP-K30, which makes the folding effect of chain polymer PEG more significant than that of PVP-K30 when forming hydrogen bonds with oxygen atoms at the same distance on the  $\text{CeO}_2$  surface.

(3) At pH values of 4, 6, 7, and 10, PVP-K30 showed stronger inhibition on  $\text{SiO}_2$  and  $\text{Si}_3\text{N}_4$  than PEG did. This is because the zeta potentials of the mixed suspension of PVP-K30 and  $\text{CeO}_2$  is smaller than that of the PEG mixed

one, which makes the suspension and  $\text{SiO}_2$  more repulsive. Moreover, PVP-K30 has a greater adsorption capacity on  $\text{SiO}_2$  and  $\text{Si}_3\text{N}_4$  surfaces than that of PEG, reducing the contact between  $\text{CeO}_2$  abrasive particles and  $\text{SiO}_2/\text{Si}_3\text{N}_4$  surfaces. At a pH value of 4, PVP-K30 showed the strongest inhibition on  $\text{Si}_3\text{N}_4$  removal, and the removal rate decreased from 81 to 9 Å/min.

As a result, it can be concluded that the performance of ceria slurries used in STI CMP process can be improved by the addition of non-ionic surfactant PVP-K30 at pH 4.

**Acknowledgements** The authors are thankful to the editors and reviewers.

**Author contribution** All authors contributed to the study conception and design. The material preparation, data collection, and analysis were performed by Lile Xie, and the first draft of the manuscript was written by Lifei Zhang. All authors commented on previous versions of the manuscript, and all authors read and approved the final manuscript.

**Funding** The research was supported by Tsinghua University Initiative Scientific Research Program.

## Declarations

**Conflict of interest** The authors declare no competing interests.

## References

- Kang HG, Park HS, Paik U et al (2011) Effects of abrasive particle size and molecular weight of poly(acrylic acid) in ceria slurry on removal selectivity of  $\text{SiO}_2/\text{Si}_3\text{N}_4$  films in shallow trench isolation chemical mechanical planarization. *J Mater Res* 22(3):777–787
- Kwak D, Oh S, Kim J et al (2021) Study on the effect of ceria concentration on the silicon oxide removal rate in chemical mechanical planarization. *Colloids Surf, A* 610:125670
- Myong KK, Byun J, Choo MJ et al (2021) Direct and quantitative study of ceria- $\text{SiO}_2$  interaction depending on  $\text{Ce}^{3+}$  concentration for chemical mechanical planarization (CMP) cleaning. *Mater Sci Semicond Process* 122:105500
- Linhardt AN, Wortman-Otto KM, Keleher JJ (2021) Evaluation of a photosensitizer redox couple for oxide removal rate tunability in shallow trench isolation chemical mechanical planarization. *ECS J Solid State Sci Technol* 10(6):063001
- Janos P, Ederer J, Pilarova V et al (2016) Chemical mechanical glass polishing with cerium oxide: effect of selected physico-chemical characteristics on polishing efficiency. *Wear* 362(363):114–120
- Prasad YN, Ramanathan S (2006) Role of amino-acid adsorption on silica and silicon nitride surfaces during STI CMP. *Electrochem Solid-State Lett* 9(12):G337–G339
- Cho CW, Kim SK, Paik U et al (2006) Atomic force microscopy study of the role of molecular weight of poly(acrylic acid) in chemical mechanical planarization for shallow trench isolation. *J Mater Res* 21(2):473–479
- Veera PRD, Peddeti S, Babu SV (2009) Selective chemical mechanical polishing of silicon dioxide over silicon nitride for shallow trench isolation using ceria slurries. *J Electrochem Soc* 156(12):H936–H943

9. Praveen B, Manivannan R, Umashankar TD et al (2014) Abrasive and additive interactions in high selectivity STI CMP slurries. *Microelectron Eng* 114(feb):98–104
10. Manivannan R, Victoria SN, Ramanathan S (2010) Mechanism of high selectivity in ceria based shallow trench isolation chemical mechanical polishing slurries. *Thin Solid Films* 518(20):5737–5740
11. Suphantharida P, Osseo-Asare K (2004) Cerium oxide slurries in CMP. Electrophoretic mobility and adsorption investigations of ceria/silicate interaction. *J Electrochem Soc* (10):151
12. Kim S, So JH, Lee DJ et al (2008) Adsorption behavior of anionic polyelectrolyte for chemical mechanical polishing (CMP). *J Colloid Interface Sci* 319(1):48–52
13. Yu L, Liu WL, Zhang ZF et al (2015) Synthesis of colloid silica coated with ceria nano-particles with the assistance of PVP. *Chinese Chemical Letters*, Chinese Chemical Society 26(6):700–704
14. Zhang J, Meng Y, Tian Y et al (2015) Effect of concentration and addition of ions on the adsorption of sodium dodecyl sulfate on stainless

steel surface in aqueous solutions. *Colloids Surf. A Physicochem Eng Asp* 484:408–415

**Publisher's Note** Springer Nature remains neutral with regard to jurisdictional claims in published maps and institutional affiliations.

This manuscript has not been published or presented elsewhere in part or in entirety and is not under consideration by another journal. We have read and understood your journal's policies, and we believe that neither the manuscript nor the study violates any of these.

Springer Nature or its licensor (e.g. a society or other partner) holds exclusive rights to this article under a publishing agreement with the author(s) or other rightsholder(s); author self-archiving of the accepted manuscript version of this article is solely governed by the terms of such publishing agreement and applicable law.